ELSEVIER

Chemical Engineering Journal 82 (2001) 95–107

Chemical Engineering Journal

www.elsevier.com/locate/cej

Design methodology and operation of a simulated moving bed reactor for the inversion of sucrose and glucose–fructose separation

Diana C.S. Azevedo[1], Alírio E. Rodrigues*

Faculty of Engineering, Laboratory of Separation and Reaction Engineering (LSRE), FEUP, University of Porto, Rua Dr. Roberto Frias S/N, 4200-465 Porto, Portugal

Received 15 May 2000; accepted 7 October 2000

Abstract

This work presents a detailed mathematical model and design methodology for a simulated moving bed reactor (SMBR) intended to invert sucrose by enzymatic action and simultaneously separate the products glucose and fructose. Experimental results for the operation of a SMBR are shown and very good agreement with simulated results was obtained. The design/optimisation package is based on an algorithm, previously developed for non-reactive SMB, used to define both the geometric parameters (column length and diameter), enzyme concentration and operating conditions of a simulated moving bed reactor. In this strategy, a detailed model is used instead of a simple equilibrium stage model. The objective of the strategy is to calculate minimum column lengths and enzyme concentrations for given feed flowrates, constrained by a reaction conversion not <99% and purities not <95% for both extract and raffinate products. Optimisation is achieved by defining the enzyme productivity as the objective function to be maximised. Design algorithm results are shown for different values of fluid/solid velocity ratios on Sections 1 and 4. This way, the effects of the safety margin applied to γ_1 and γ_4 have been investigated on the reaction conversion and separation performance. The results have been compared with predictions from the equilibrium theory for a non-reactive system and the observed deviations have been evidenced and discussed.

Keywords: Simulated moving bed reactor; Sucrose inversion; Glucose; Fructose

1. Introduction

The combination of a chemical reaction and a chromatographic separation process in a single unit operation may improve the course of reaction as well as the separation efficiency. Higher conversions and better yields can be achieved by separating unreacted reagents from products of an equilibrium reaction. In bioreactors, for instance, many biologic reactions catalysed by micro-organisms are efficient when operated with product concentration within a certain physiologic range [1]. Besides, a build-up of product concentration may lead to inhibition of the process concerned and thus, limit productivity. Other practical reasons in favour of the combination of reaction and separation in a single step are a better use of the adsorbent/catalyst bed and reduction in solvent requirements.

Perhaps, one of the most interesting physical implementations of a chromatographic reactor-separator is the simulated moving bed reactor. In such a reactor, reaction occurs either in the mobile or stationary phase. In the latter, the catalyst is supported or immobilised in the solid adsorbent, which promotes the separation of the reaction products. The countercurrent motion of the stationary phase is simulated by applying an intelligent scheme of valve switchings on a set of fixed beds. Some continuous reaction/separation chromatographic processes by SMBR have been successfully reported in the literature, such as:

- The inversion of sucrose and subsequent separation of the obtained invert sugar (glucose + fructose) [2].
- The oxidative coupling of methane with subsequent separation and recycling of unreacted methane [3].
- The esterification from acetic acid and β-phenethyl alcohol and subsequent separation of the product β-phenetyl acetate [4].
- The synthesis and separation of methanol from syngas [5].

In the biochemical field, other ingenious arrangements that implement the principle of continuous chromatographic reaction/separation principle have been reported. Ganetsos and co-workers [6,7] have successfully used a continuous countercurrent chromatographic reactor–separator

* Corresponding author. Tel.: +351-22-508-1671; fax: +351-22-508-1674.
E-mail address: arodrig@fe.up.pt (A.E. Rodrigues).
[1] On leave from: Department of Chemical Engineering, Federal University of Ceará, GPSA, Brazil.

1385-8947/01/$ – see front matter
PII: S1385-8947(00)00359-4

Nomenclature

A	column section area (m^2)
C	fluid phase concentration, mol per void volume in bed
C^{in}	bed inlet concentration ($mol\,m^{-1}$)
$\bar{C}_p$	mean pore concentration (mol per fluid volume in particle pores)
d_p	resin particle diameter (m)
k_f	film mass transfer coefficient ($m\,s^{-1}$)
k_p	mass transport coefficient in the pores (s^{-1})
k_μ	mass transport coefficient in the microparticles (s^{-1})
k_r	Reaction rate constant from Michaelis–Menten equation (s^{-1})
K	equilibrium constant ((mol adsorbed/particle volume)/(fluid volume in particle pores/mol in pore fluid phase))
K'	equilibrium constant for a homogeneous adsorbent particle ((mol adsorbed/particle volume)/ (void volume in bed/mol in bed fluid phase))
L_b	column length (m)
L_j	zone length (m)
$\langle\bar{q}\rangle$	mean solid phase concentration averaged over the particle (bi-LDF approximation) (mol adsorbed/particle volume)
Q	SMB fluid flowrate ($m^3\,s^{-1}$)
Q'	TMB fluid flowrate ($m^3\,s^{-1}$)
R_p	particle radius (m)
t^*	rotation period (s)
U_F	fluid interstitial velocity ($m\,s^{-1}$)
U_S	solid interstitial velocity ($m\,s^{-1}$)
v	fluid superficial velocity ($m\,s^{-1}$)
V_b	column volume (m^3)

Greek letters

α_p	number of macropore mass transfer units (bi-LDF approximation)
α_μ	number of microparticle mass transfer units (bi-LDF approximation)
α_r	number of reaction units
β	safety margin used to calculate γ_1 and γ_4
ε	bed porosity, dimensionless
ε_p	particle porosity, dimensionless
ν	solid/fluid volume ratio
Ω	scale factor

Subscripts and superscripts

1, 2, 3, 4	referring to TMB zones
b	bed
eq	conditions defined in the equilibrium
F, R, E, X	feed, raffinate, eluent and extract SMB streams, respectively
FR	fructose
GL	glucose
i	chemical species (fructose or glucose)
j	TMB/SMB section
k	SMB column
p	particle
sp	specified

(SCCR-S) for the inversion of sucrose and biosynthesis of dextran from sucrose. Sardimi and Barker [8] were the first authors to carry out the inversion of sucrose and separation of fructose from glucose using a continuous rotating annular chromatograph (CRAC). Hashimoto and co-workers [9] studied the use of a continuous moving-column chromatographic separator for the production of high-fructose syrups by combining the adsorption of fructose and isomerisation of the separated glucose fraction on alternatively arranged adsorption and bio-reaction columns.

The inversion of sucrose and subsequent separation of produced glucose and fructose by continuous chromatographic reactor–separators have been studied mainly by the groups from the University of Dortmund [2] and Aston [7,8]. There are few experimental results published except for the use of separator–reactor of CRAC and SCCR-S types. The inversion of sucrose by enzyme invertase, represented below, is an irreversible reaction, and thus, the reaction rate is not influenced by product accumulation.

$$\text{Sucrose} \overset{\text{invertase}}{\rightarrow} \text{Fructose} + \text{Glucose}$$

However, it has been shown that, even for irreversible reactions, the use of a SMBR increases conversion and product purity as compared to the performance of an equivalent chromatographic reactor–separator in batch mode [2]. Barker et al. [7] have also shown that simultaneous inversion and product separation makes it possible to overcome problems associated with substrate inhibition.

The design and optimisation of an SMBR to carry out simultaneous and continuous bio-reaction and separation are essential to define the feasibility of implementation of the process at industrial scale. Although the number of publications focusing on the design of non-reactive SMB's is quite large [10–13], the same may not be said of SMBR design [14,15]. Design will define geometric and operating parameters that should lead not only to product separation, but also to high reagent conversions. If the reaction is to be catalysed, and this is the case in bio-reactions, the amount of catalyst is an additional degree of freedom to the optimisation problem. This work proposes a design methodology for SMB reactors based on an existing design strategy for non-reactive SMB's, as proposed by Biressi et al. [16]. The methodology employs a detailed process model instead of the equilibrium-staged model, used by Biressi. Its results are further used to optimise the enzyme and adsorbent inventories so as to obtain a desired performance at minimum cost.

The effect on the optimisation results of the safety margin used on the velocity ratios of the SMBR regeneration sections (Sections 1 and 4) is also shown. Experimental results are presented so as to validate the process model used in the design methodology.

2. Simulated moving bed reactor model

The model to be presented in this section is based on the description of a true moving bed reactor (TMBR), which should be equivalent to an actual simulated moving bed reactor (SMBR). In a real simulated moving bed reactor, there is a set of fixed beds connected in a closed circuit through which flows a continuous recycling flowrate. Consider the irreversible catalysed reaction $A \rightarrow B + C$, where B is preferentially adsorbed in the adsorbent which packs the SMBR beds. The SMBR inlet streams are the eluent (containing the enzyme/catalyst) and the feed (containing A). The outlet streams are the B-rich extract and C-rich raffinate. They should be pumped into/out of the unit at certain positions, which shift simultaneously one bed in the direction of fluid flow. Reaction occurs in Section 3, between feed and raffinate nodes, while one of the reaction products, B, is preferentially retained by the packed adsorbent. Therefore, C is collected at the raffinate node at high purity. B is to be collected at high purity in the extract node after being eluted by the eluent.

Fig. 1 shows a schematic drawing of a real simulated moving bed reactor. An equivalent situation would be obtained by moving the solid adsorbent countercurrently to the fluid phase, as also shown in Fig. 1. The inlet and draw-off points would be fixed, instead, and a true moving bed reactor (TMBR) would be obtained. Table 1 summarises the relations of equivalence between a TMBR and a SMBR.

Table 1
Equivalence relations between a simulated moving bed reactor (SMBR) and a true moving bed reactor (TMBR)

	SMBR	TMBR
Solid phase		
Velocity	0	$U_s = L_b/t^*$
Flowrate	0	$Q_s = U_s(1-\varepsilon)A$
Liquid phase		
Velocity	U_{fk}	$U'_{Fj} = U_{Fk} - U_s$[a]
Flowrate	Q_k	$Q'_j = Q_k - \varepsilon V_b/t^*$[a]

[a] Equivalence for a SMB column k belonging to a section j.

The modelling of a TMBR is much simpler than the modelling of a SMBR since the equations are reduced to those of four countercurrent beds and steady-state equations may be applied straight away. For the reaction/separation system considered in this work, the reagent A is sucrose, B and C are fructose and glucose, respectively. The catalyst is enzyme invertase, which is diluted in the eluent in free form.

For each of the four countercurrent sections of a TMBR (denoted by subscript j), the differential mass balance equations for chemical species (i) at steady-state would be the following:

- For the bed fluid phase between adsorbent particles

$$\frac{\gamma_j}{Pe_j}\frac{d^2C_{i,j}}{dx^2} - \gamma_j\frac{dC_{i,j}}{dx} - \nu\frac{Bi_{mj}}{Bi_{mj}+5}\alpha_{pi,j}(C_{i,j} - \bar{C}_{pi,j}) + \alpha_{rj}(1+\nu K_e)\left(\frac{\sigma_i R_j}{k_r}\right) = 0, \quad i = \text{glucose or fructose} \tag{1}$$

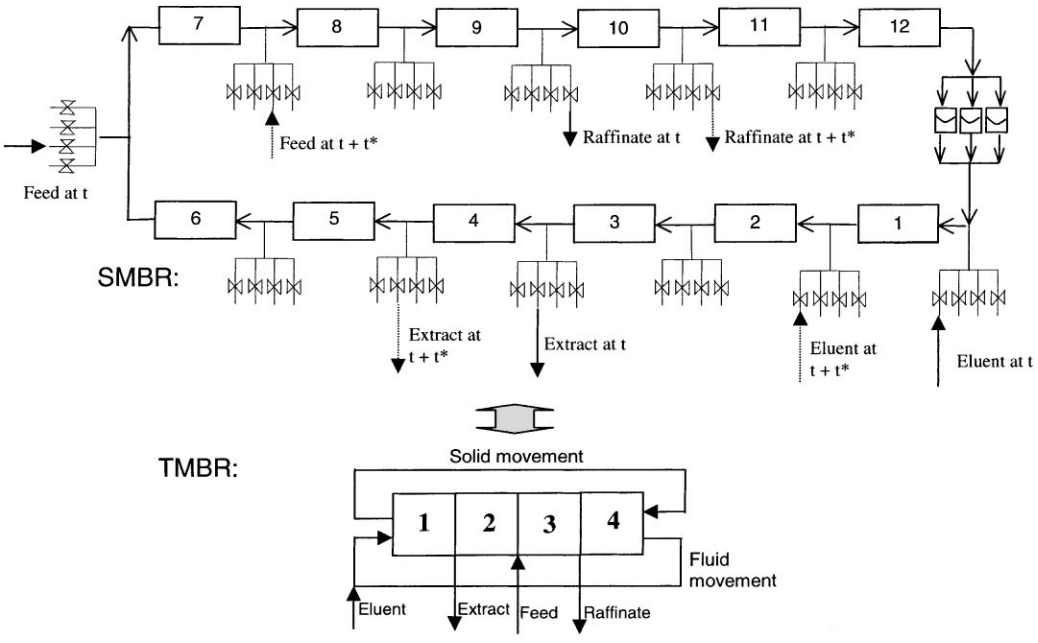

Fig. 1. Schematic drawings of a simulated moving bed reactor (SMR) and a true (countercurrent) moving bed reactor (TMBR).

$$\frac{\gamma_j}{Pe_j}\frac{d^2C_{i,j}}{dx^2} - \gamma_j\frac{dC_{i,j}}{dx} + \alpha_{rj}(1+\nu K_e)\left(\frac{\sigma_i R_j}{k_r}\right) = 0,$$
i = sucrose (2)

$$\frac{1}{Pe_j}\frac{d^2C_{i,j}}{dx^2} - \frac{dC_{i,j}}{dx} = 0, \quad i = \text{enzyme} \tag{3}$$

where $R_j = k_r\dfrac{C_{s,j}\times C_{e,j}}{K_{mm}+C_{s,j}}$;

$$\sigma_i = \begin{cases} -1, \text{ if } i = \text{sucrose} \\ +0.526, \text{ if } i = \text{glucose or fructose} \end{cases} \tag{4}$$

and K_e is linear adsorption constant of enzyme onto resin surface.

- For the fluid phase within particle pores (i is glucose or fructose, only)

$$\frac{\partial\bar{C}_{pi,j}}{\partial x} + \frac{Bi_{mj}}{5+Bi_{mj}}\frac{\alpha_{pj}}{\varepsilon_p}(C_{i,j}-\bar{C}_{pi,j}) - \frac{\alpha_{\mu j}}{\varepsilon_p}[K_i\bar{C}_{pi,j} - \langle\bar{q}\rangle_{i,j}] = 0 \tag{5}$$

- For the solid phase within the resin particles (i is glucose or fructose, only)

$$\frac{\partial\langle\bar{q}\rangle_{i,j}}{\partial x} + \alpha_{\mu j}[K_i\bar{C}_{pi,j} - \langle\bar{q}\rangle_{i,j}] = 0 \tag{6}$$

The corresponding boundary conditions for a given section j are

$$C^{in}_{i,j} = C_{i,j}(0) - \frac{1}{Pe_j}\frac{\partial C_{i,j}}{\partial x}, \quad \text{for any } i \tag{7}$$

$$\frac{\partial C_{i,j}}{\partial x}(1) = 0, \quad \text{for any } i \tag{8}$$

$$\bar{C}_{pi,j}(1) = \bar{C}_{pi,j+1}(0), \quad \text{for } i = \text{glucose or fructose} \tag{9}$$

$$\langle\bar{q}\rangle_{i,j}(1) = \langle\bar{q}\rangle_{i,j+1}(0), \quad \text{for } i = \text{glucose or fructose} \tag{10}$$

The dimensionless space variable is $x = z/L_j$, where L_j is the length of section j. The dimensionless numbers present in the model equations are

$$\gamma_j = \frac{U'_{Fj}}{U_S} \quad \text{fluid/solid intersticial velocity ratio} \tag{11}$$

$$Pe_j = \frac{U'_{Fj}L}{D_{axj}} \quad \text{Peclet number} \tag{12}$$

$$\nu = \frac{(1-\varepsilon)}{\varepsilon} \quad \text{solid/fluid phase ratio} \tag{13}$$

$$\sigma_i = \frac{\text{mol. weight of species } i}{\text{mol. weight of sucrose}} \tag{14}$$

$$\alpha_{pj} = \frac{k_p L_j}{U_S} \quad \text{number of macropore mass transfer units} \tag{15}$$

$$\alpha_{rj} = \frac{k_r L_j}{U_S} \quad \text{number of reaction units} \tag{16}$$

$$\alpha_{\mu j} = \frac{k_\mu L_j}{U_S} \quad \text{number of microparticle mass transfer units} \tag{17}$$

$$Bi_{mj} = \frac{k_{fj}R_p}{D_{pe}}k \quad \text{mass Biot number} \tag{18}$$

$C^{in}_{i,j}$, present in the boundary condition at the section inlet, can be found from the node balances. The following equations are valid for all i (glucose, fructose, sucrose and enzyme)Eluent node

$$C^{in}_{i,1} = \frac{Q'_4}{Q'_1}C_{i,4}(1) + \frac{Q_E}{Q'_1}C_{i,E} \tag{19}$$

Extract node

$$C^{in}_{i,2} = C_{i,1}(1) \tag{20}$$

Feed node

$$C^{in}_{i,3} = \frac{Q'_2}{Q'_3}C_{i,2}(1) + \frac{Q_F}{Q'_3}C_{i,F} \tag{21}$$

Raffinate node

$$C^{in}_{i,4} = C_{i,3}(1) \tag{22}$$

The reaction of inversion of sucrose was described by the Michaelis–Menten equation, as stated in Eq. (4). Since all mass balance equations are written in terms of mass rather than moles, the "stoichiometric" parameter σ_i is calculated as the ratio between the molecular weight of species i and that of sucrose.

Sucrose is assumed to react in inter-particle fluid phase and at the surface of the resin due to immobilized enzyme adsorbed at its exterior surface. This is accounted for by the term $(1+\nu K_e)$, present in Eqs. (1) and (2). Reaction products glucose and fructose are assumed to have linear isotherms, as measured in previous publications [17–19]. Their diffusion within the adsorbent particle is described by means of a bi-linear driving force approximation, described elsewhere [20]. Sucrose adsorption into the adsorbent particles was not considered in the model, since we have observed experimentally that the adsorption constant of sucrose is nearly equal to the particle porosity [21]. Diffusion of sucrose into the adsorbent was not considered as well since the reaction characteristic time constant ($50.32\,\text{min}^{-1}$), as measured by Santos [21], is much larger than the pore diffusion characteristic time ($1.44\,\text{min}^{-1}$), as calculated from the Glueckauf correlation.

The system of ordinary differential equations that describes the process was solved numerically, using the ODE solver package COLNEW [22]. Spatial discretization was performed by modified B-splines assuming 150 elements per section with two collocation points in each element. The

integrator tolerance was set at 10^{-9}. Solution was pursued by consecutive iterations, each new iteration taking the solution calculated from the previous one as an initial guess. This recursive process went on until the sum of the following absolute errors was less 1%:

1. Sum of relative differences between extract and raffinate concentrations of two consecutive iterations.
2. Global molar balance between sucrose and invert sugar (for each mole of sucrose that enters the SMBR, 1 mol of glucose and 1 mol of fructose must leave).
3. Global mass balance for enzyme (amount that enters equal to amount that leaves).

The solver took an average of 12 iterations to solve the system of ODE's. Run times were typically 2–3 min in a Pentium II 300 MHz processor.

Table 2
Model parameters and operating conditions used in the SMBR experiment for inversion of sucrose and fructose–glucose separation

Model parameters	Operating conditions	Columns
$Pe = 1500$	$T = 55^{\circ}C$	$D_b = 2.6\,cm$
$Bi_m = 500$	pH = 4.5	$L_b = 29\,cm$
$k_r = 50.32\,min^{-1}$	$C_F = 80\,g$ sucrose per liter buffer[a]	Configuration: 3-2-5-3
$K_{mm} = 23\,g\,l^{-1}$	$C_e = 250\,mg\,l^{-1}$ buffer[a]	$d_p = 320\,mm$
$k_p = 2.5\,min^{-1}$	$t^* = 3.4\,min$	$\gamma_1 = 0.95$
$k_\mu = 1.5\,min^{-1}$	$Q_{Rec} = Q_4 = 24\,ml\,min^{-1}$	$\gamma_2 = 0.45$
$K_{FR} = 0.43$	$Q_E = 11.38\,ml\,min^{-1}$	$\gamma_3 = 0.65$
$K_{GL} = 0.17$	$Q_F = 3.62\,ml\,min^{-1}$	$\gamma_4 = 0.33$
$K_e = 5$	$Q_R = 5.89\,ml\,min^{-1}$	
$\epsilon_p = 0.1$	$Q_X = 9.11\,ml\,min^{-1}$	

[a] Feed concentration.

3. Experimental results

A simulated moving bed reactor has about the same physical configuration as a simulated moving bed separator. Catalytic reaction is possible by either immobilising the catalyst on the solid adsorbent or introducing it in free form together with the eluent/dessorbent. A SMBR experiment was carried out at a SMB pilot unit LICOSEP (by Novasep) using 12 columns (290 mm × 26 mm, length × i.d.). The columns were packed with the cation-exchange resin DOWEX Monosphere 99/Ca, by Sigma, with a particle diameter of 320 μm. The chosen section configuration was 3, 2, 5 and two columns for Sections 1–4, respectively. This choice was made based on previous experimental work conducted by LSRE [21]. Section 3, where reaction and adsorption of one of the reaction products take place, should be longer than the other sections. Sections 2 and 4, where the weakly adsorbed component is desorbed and adsorbed, respectively, may be shorter than the other sections.

The feed was a diluted sucrose solution (8 g per 100 ml), since the Michaelis–Menten equation has been shown to apply [21] at this concentration. Besides, the available SMB equipment could not withstand the high pressure drops that would result from the high viscosity of concentrated sucrose syrups due to the small diameter of tubing (1/16″) connecting columns. The enzyme invertase, which catalyses the inversion of sucrose, was fed to the SMBR diluted in the eluent. Its maximum activity is observed at 55°C and pH 4.5, according to the supplier. Therefore, the eluent consisted of a pH 4.5 buffer prepared from acetic acid (0.28% v/v) and calcium acetate (0.5% w/v). Calcium acetate was used instead of other buffering salts not to alter the adsorbent resin ionic form and maintain its adsorption properties. The sucrose solution used as feed was also prepared with this buffer, so that the pH of the whole mobile phase present in the SMBR would be 4.5 throughout the experiment. Temperature was kept at 55°C, by keeping the eluent and feed reservoirs in a thermostatic bath and by circulating bath water through the column jackets. Eventual acid hydrolysis in the feed reservoir was monitored by HPLC analysis of samples of feed in the beginning and at the end of the experiment. No appreciable sucrose degradation was observed.

Adsorption equilibrium data, mass transfer and reaction parameters for sucrose inversion and glucose–fructose adsorptive separation are shown in Table 2. Together with the column axial dispersion, these parameters were measured in our laboratory, the experimental procedure being described elsewhere [23]. The external mass transfer coefficient (used to calculate Bi_m) was estimated from literature correlations for fixed beds [24]. The linear adsorption constant of the enzyme on the resin, K_e, was measured experimentally by calculating the stoichiometric time of enzyme breakthrough curves. These curves were obtained by registering the UV signal at the outlet of a SMB column subject to steps in enzyme concentration.

Table 2 also summarises the operating conditions (flowrates and switching time) used in the experiment. The experiment was intended to demonstrate the validity of the proposed model for a SMBR. Therefore, operating conditions were cautiously selected so as to provide a high conversion and good separation of products. By comparing the reaction time constant, k_r, with the mass transfer time constants, k_p and k_μ, one may foresee that reaction is much faster than product (glucose and fructose) diffusion in the resin. Hence, the equilibrium model concept, formulated for linear equilibrium non-reactive systems [25], was used as an initial guess to provide adequate values for the TMBR section velocity ratios according to the following equations:

$$\gamma_1 > \gamma_1^{eq} \text{ and } \gamma_1^{eq} = \nu(K_{FR} + \varepsilon_p) = 0.8, \text{ therefore,}$$
$$\gamma_1 = 0.953 \quad (23)$$

$$\gamma_2^{eq} < \gamma_2 < \gamma_3 < \gamma_3^{eq} \text{ and } \gamma_2^{eq} = \nu(K_{GL} + \varepsilon_p)$$
$$= 0.405 \text{ and } \gamma_3^{eq} = \nu(K_{FR} + \varepsilon_p) = 0.8 \quad (24)$$

$$\text{therefore } \gamma_2 = 0.45 \text{ and } \gamma_3 = 0.65 \quad (25)$$

$\gamma_4 < \gamma_4^{eq}$ and $\gamma_4^{eq} = \nu(K_{GL} + \varepsilon_p) = 0.405$, therefore,

$$\gamma_4 = 0.325 \quad (26)$$

The recycling pump of the SMB unit could deliver flowrates in the range of 20–120 ml min^{-1}. The adsorbent inventory being much smaller than that usually reported for fructose–glucose SMB separations, lower flowrates were required in order to overcome mass transfer resistance. A flowrate of 24 ml min^{-1} was assumed for Section 4, the zone having the lowest flowrate. Having set γ_4 as 0.325, the switching time t^* could be calculated from Eq. (27) and was equal to 3.4 min.

$$\gamma_j = \frac{Q_j t*}{\varepsilon V_b} - 1 \quad (27)$$

All the other section flowrates were calculated using Eq. (27). The inlet and outlet streams were calculated from the differences between neighbouring section flowrates. The amount of enzyme necessary to completely convert the feed was calculated based on the activity information provided by the supplier. Each mg of enzyme contains 46 units. One enzyme unit is defined as the amount necessary to invert 1 μmol of sucrose per minute at 55°C and pH 4.5. The feed flowrate is 3.62 ml min^{-1} and sucrose concentration is 80 g l^{-1}, which means a throughput of 846.8 μmol min^{-1}. To invert such amount, 846.8 enzyme units or 18.4 mg would be necessary within the SMBR void volume. The total SMBR void volume is $12 \times 0.4 \times 154 \approx 740$ ml, thus the enzyme concentration must be 0.025 g l^{-1}. The definition of enzyme activity is usually calculated for a condition in which the substrate concentration is much larger than the Michaelis–Menten constant. In such condition, the rate of reaction is constant and maximum. Since concentrations of sucrose comparable to the Michaelis–Menten constant (23 g l^{-1}) were used in the SMBR, the enzyme activity at such condition will probably be lower and more enzyme will be required to achieve the same conversion rate. That is why, we arbitrarily set the amount of enzyme in the eluent as 10 times the theoretical amount as given by the supplier information, i.e. 0.25 g l^{-1}.

During the first cycle of operation, enzyme with diluted buffer was pumped into the SMBR by both eluent and feed pumps in order to make sure that mobile phase and resin were saturated with catalyst. From the second cycle on, the feed pump started delivering sucrose solution. At each cycle, raffinate and extract were collected and analysed by HPLC for sugar content assessment in order to monitor the steady-state attainment. Stationary average product concentrations were obtained at the 10th cycle. In the 15th cycle, 1 ml samples were collected at 50% of each of the 12 periods with the aid of a six-port valve. The samples were immersed in boiling water for 1 min in order to ensure the inactivation of the enzyme and stop reaction. Fig. 2(a) shows the obtained experimental profile (points) as compared with the simulated curves. Very good agreement is found in between the theory and experiment. Sucrose is completely converted

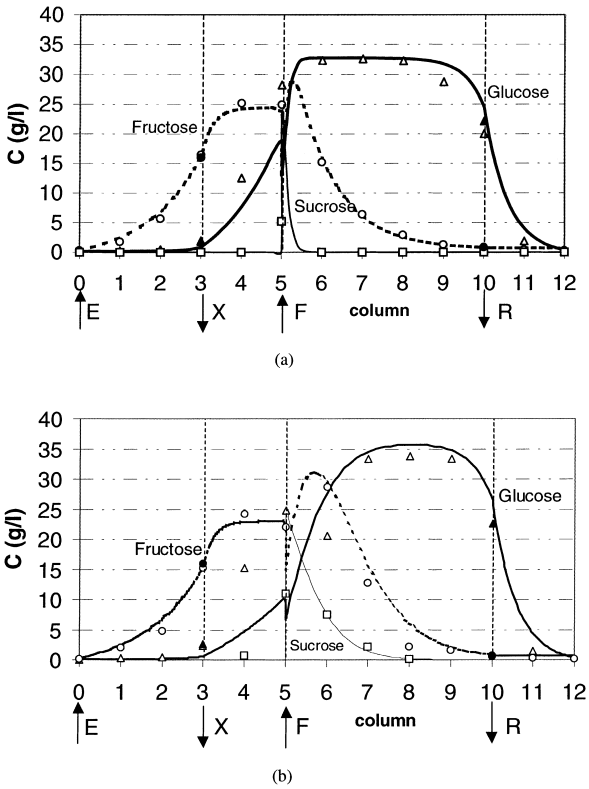

Fig. 2. (a) Axial concentration profile for a simulated moving bed reactor at steady-state operating under conditions summarised in Table 2. Curves indicate simulated results (dotted line for fructose, continuous thick line for glucose and continuous thin line for sucrose). Blank (white) points indicate concentration of samples collected at 50% of each period. Filled (black) points indicate average product concentrations collected for a whole cycle. (b) The same as for the previous figure, with $\gamma_2 = 0.43$, $\gamma_3 = 0.63$ and enzyme concentration of 40 mg l^{-1}.

within the first of the five columns that make up Section 3. One would think that such a long section is not necessary to achieve 100% conversions. However, fructose, one of the reaction products which is preferentially adsorbed, diffuses slowly within the resin. Thus, it takes the whole section length for fructose concentration to decrease to nearly zero, so as not to contaminate the raffinate stream. At the raffinate and extract nodes, the filled points indicate the average concentrations measured for both products collected for a whole cycle (15th cycle).

Table 3 compares the performance parameters obtained experimentally with those predicted by the numerical simulation. Experimental performance is slightly different from the predicted one. This may be due to the use of the equivalent true moving bed reactor (TMBR) model instead of an actual SMBR and to small deviations in the flowrates delivered by the recycling pump. However, such error may be accepted if the model is to be used for design/optimisation purposes, given its simplified solution.

Another experiment was performed using a lower enzyme concentration, 40 mg l^{-1}, in order to make more effective use of Section 3 as a reactor. The operating conditions are

Table 3
Predicted vs. experimental performance parameters obtained in SMBR experiment

Performance parameter	Experimental	Predicted
Extract purity (%)	90	92.6
Raffinate purity (%)	96.3	96.1
Extract productivity ($kg\,m^{-3}\,h^{-1}$)	7.78	7.55
Raffinate productivity ($kg\,m^{-3}\,h^{-1}$)	7.07	7.40
Enzyme productivity (kg sucrose per gram enzyme)	0.102	0.102
Fructose conc. in extract ($kg\,m^{-3}$)	15.78	15.3
Glucose con. In raffinate ($kg\,m^{-3}$)	22.18	23.2

nearly the same as described in Table 2, except for the extract and raffinate flowrates, which were equal to 9.47 and $5.53\,ml\,min^{-1}$, respectively. Hence, $\gamma_2 = 0.43$ and $\gamma_3 = 0.63$. Fig. 2(b) shows the steady-state experimental axial profile as compared with the model predictions. The decrease in enzyme concentration caused the sucrose concentrations to be positive for three columns of Section 3. It is possible to verify the adequate description of the reaction rate from the nice agreement between theory and experiment.

4. Design of a simulated moving bed reactor

The strategy design for a SMBR proposed in this work consists in determining the column dimensions (length and section), enzyme concentration and operating conditions that allow a desired substrate conversion and purity in the outlet streams with the maximum enzyme productivity and without exceeding given pressure drop limits imposed by the packing material. The number of degrees of freedom in the design problem is, therefore, 8: column length and diameter, enzyme concentration, switching time and the four section velocity ratios of γ_j. The optimisation algorithm to be applied is an extension of that developed by Biressi et al. [16] for non-reactive SMB's. However, instead of using an equilibrium stage model, we have used a detailed TMBR model, as shown and validated in the previous section.

The equations from an equilibrium model that define separation for a non-reactive linear SMB will be used as general guidelines to define adequate values for γ_j. Those equations are

$$\gamma_1 > \nu K'_{FR} \tag{28}$$

$$\nu K'_{GL} < \gamma_2 < \nu K'_{FR} \tag{29}$$

$$\nu K'_{GL} < \gamma_3 < \nu K'_{FR} \tag{30}$$

$$\gamma_4 < \nu K'_{GL} \tag{31}$$

where $\nu = (1-\varepsilon)/\varepsilon$ and $\gamma_3 > \gamma_2$.

As shown by Migliorini et al. [15], a complete conversion/separation region has a more reduced triangular shape, similar to that found for non-reactive SMB's. This was said of non-linear adsorption system in which feed concentration is a key optimisation parameter. We have assumed this conclusion to be true for our reaction/separation system.

The pieces of information to be used in our design/optimisation algorithm are:

1. A correlation to estimate pressure drop in packed beds, such as the Kozeny–Kárman equation

$$\frac{\Delta P}{L_b} = 150\frac{(1-\varepsilon)^2}{\varepsilon^3 d_p^2}\mu v \tag{32}$$

2. The separation region for a non-reactive SMB in the operating parameters space as defined by the equilibrium theory (Eqs. (28)–(31)).
3. The detailed TMBR model as proposed previously, together with the equivalence relations between a TMBR and a SMBR.
4. The theoretical calculation of the necessary amount of enzyme within the SMBR volume, according to the supplier's information about the enzyme activity.

As a first step of the optimisation procedure, the following three statements are made, as adapted from the work of Biressi et al. [16].

1. The SMBR flowrate in Section 1, Q_1, is taken to be $10^3\,ml\,min^{-1}$, and all other flowrates and column cross-section are calculated having this value in mind. After the algorithm calculations are finished, a scale parameter Ω is obtained as the ratio between the desired feed flowrate and the calculated feed flowrate with $Q_1 = 10^3\,ml\,min^{-1}$, i.e. $\Omega = Q_F$ (desired)/Q_F ($Q_1 = 10^3\,ml\,min^{-1}$). All other calculated flowrates and section area may be multiplied by the scale factor to obtain the values necessary to process the desired feed flowrate. Calculated γ_j and L_b values remain unchanged.
2. Since, pressure drop is proportional to the throughput of the plant, we expect that the productivity will be the highest when pressure drop is the highest possible in the plant. Therefore, we set pressure drop in Section 1, which is where the fluid velocity is maximum, equal to the allowable upper limit, hence, fixing the value of the product $v_1 \times L_b$.
3. From the adsorption isotherms and using a certain safety margin β, it is possible to predict a priori the values of γ_1 and γ_4 which guarantee the proper behaviour of Sections 1 and 4, that is, complete regeneration of the adsorbent and eluent, respectively. β is an input parameter to the algorithm so that $\gamma_1 = \beta \times \gamma_1^{eq}$ and $\gamma_4 = \gamma_4^{eq}/\beta$. Design results for different values of β are analysed.

From the items described above, Q_1, $v_1 \times L_b$, γ_1 and γ_4 are defined. Four from the initially 8 d.f. of the design problem are left to be defined: the column length, enzyme concentration and the velocity ratios γ_2 and γ_3. To define the most adequate values for these variables, an optimisation algorithm is proposed having both reaction conversion

and product purities as constraints. The objective function is enzyme productivity, which should be maximised. The constraints reaction conversion (X), extract purity (PUX), raffinate purity (PUR) are defined as follows:

$$X = \frac{\text{sucrose in the feed} - \text{sum of sucrose in the extract and raffinate}}{\text{sucrose in the feed}} \times 100 \quad (33)$$

$$PUX = \frac{\text{fructose in the extract}}{(\text{fructose} + \text{glucose}) \text{ in the extract}} \times 100 \quad (34)$$

$$PUR = \frac{\text{glucose in the raffinate}}{(\text{fructose} + \text{glucose}) \text{ in the raffinate}} \times 100 \quad (35)$$

The parameter η will be used in the algorithm and is defined as the dimensionless distance of a certain (γ_2, γ_3) pair to the optimum point given by the equilibrium theory (γ_2^{eq}, γ_3^{eq}). In other words

$$\eta = \frac{\gamma_3 - \gamma_2}{\gamma_3^{eq} - \gamma_2^{eq}} = \frac{\gamma_3 - \gamma_2}{\nu\,(K_{FR} - K_{GL})} \quad (36)$$

For each value of η, within a certain range defined by the user, the algorithm manages to find the minimum column length, minimum enzyme concentration and γ_2, which lead to the required reaction conversion and product purities. For a given value of η, the algorithm starts with the minimum (γ_2, γ_3) pair defined by the non-reactive equilibrium triangle and sufficiently small values for L_b and C_e. All information required by the TMBR model is available by then and process performance is calculated. Depending on the values of the constraining parameters (reaction conversion and product purities), the algorithm makes one of the following decisions:

- increase enzyme concentration;
- increase column length;
- increase/decrease (γ_2, γ_3).

The flow sheet describing the decision-making process of the algorithm is visualised in Fig. 3.

With the data stored by the design package, plots of η versus column length and enzyme productivity are constructed. The value of η which maximises productivity is chosen as

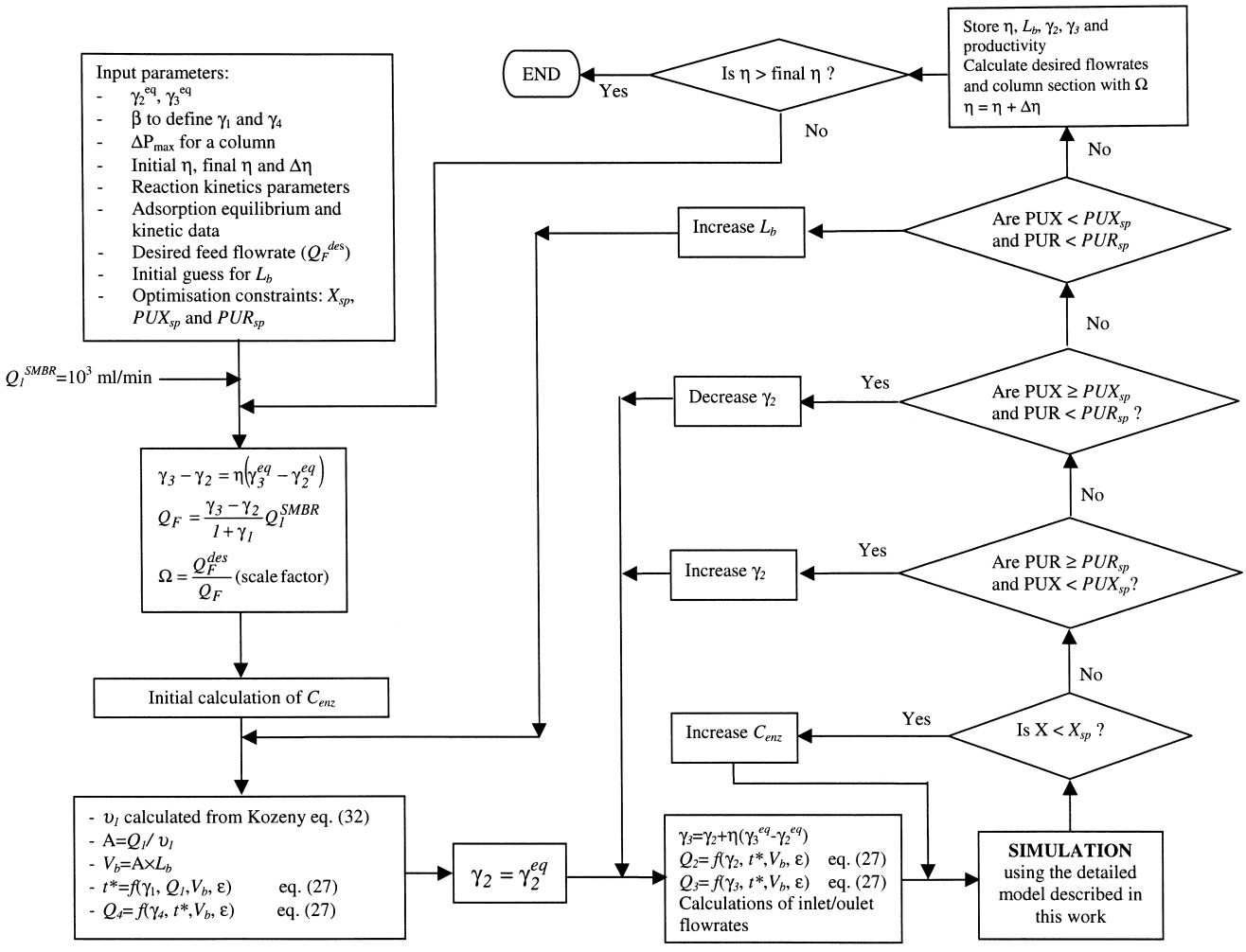

Fig. 3. Flow sheet of the algorithm used to design SMBR dimensions, enzyme concentration and operating conditions.

the adequate operating point. It defines the optimum column length, optimum enzyme concentration and the scale factor Ω. Multiplying the obtained section area and flowrates by Ω, one is able to re-scale all necessary operating conditions for any desired throughput.

5. Design methodology results

The design methodology was applied for a SMBR to invert sucrose and separate glucose from fructose. Equilibrium, mass transfer and reaction parameters are those shown in Table 2. For a feed concentration of $400\,g\,l^{-1}$, fluid viscosity and density were found to be 3 cP and $1.26\,kg\,l^{-1}$, respectively [26]. The maximum pressure limit was set at 10 bar per column, 25% of such value being due to the column packing itself and 75% being due to piping and valves. The safety margin β to be used in the calculation of γ_1 and γ_4 was set as 1.1, 1.2 and 1.3 in order to verify the influence of this parameter in the design/optimisation results.

Fig. 4 shows the plots of η as a function of minimum length, minimum C_e and productivities that lead to a minimum conversion of 99% and minimum purities of 95%. In this plot, sucrose concentration in the feed was $400\,g\,l^{-1}$ and $\beta = 1.1$. Fig. 4(a) shows the evolution of enzyme productivity with η. The maximum value of the curve is located at $\eta = 0.5$. However, at this value of η, low feed flowrates are treated by the SMBR, which means low product concentration and low adsorbent productivities. One may also verify that, from $0.4 < \eta < 0.8$, enzyme productivity values are located on a plateau above 2.5 kg sucrose per g of enzyme. Both column length and adsorbent productivity increase steadily for the η range considered in the algorithm. From $\eta = 0.8$ on, the required amount of enzyme (plot b) increases with a greater slope. Therefore, for $\beta = 1.1$, the best range of operation point for a SMBR seems to lie anywhere between $\eta = 0.4$ and $\eta = 0.8$. Figs. 5 and 6 show the same type of plots as in Fig. 4, with β equal to 1.2 and 1.3, respectively. Similar conclusions as those drawn from Fig. 4 may be stated. For β equal to 1.2, the ideal operating range is also located at $0.4 < \eta < 0.8$. For β equal to 1.3, this interval is enlarged to (0.3, 1.0). For the same η, the minimum column length required to achieve the specified process performance decreases as β increases. This is expected since larger values of β mean better eluent and adsorbent regeneration and hence, shorter section lengths are necessary to achieve the same performance. Although the highest enzyme productivities are obtained for β equal to 1.1, SMBR operation at low β values is not recommended because it may not be robust enough. Operating at very high values of β is not advisable as well, since very low enzyme productivities and diluted product concentrations may be obtained. The figures of ideal operating ranges for diverse values of η are summarised in Table 4. In order to have a robust operation and not to obtain very diluted products, it would be wise to operate the SMBR at $\beta = 1.2$ and $\eta = 0.8$.

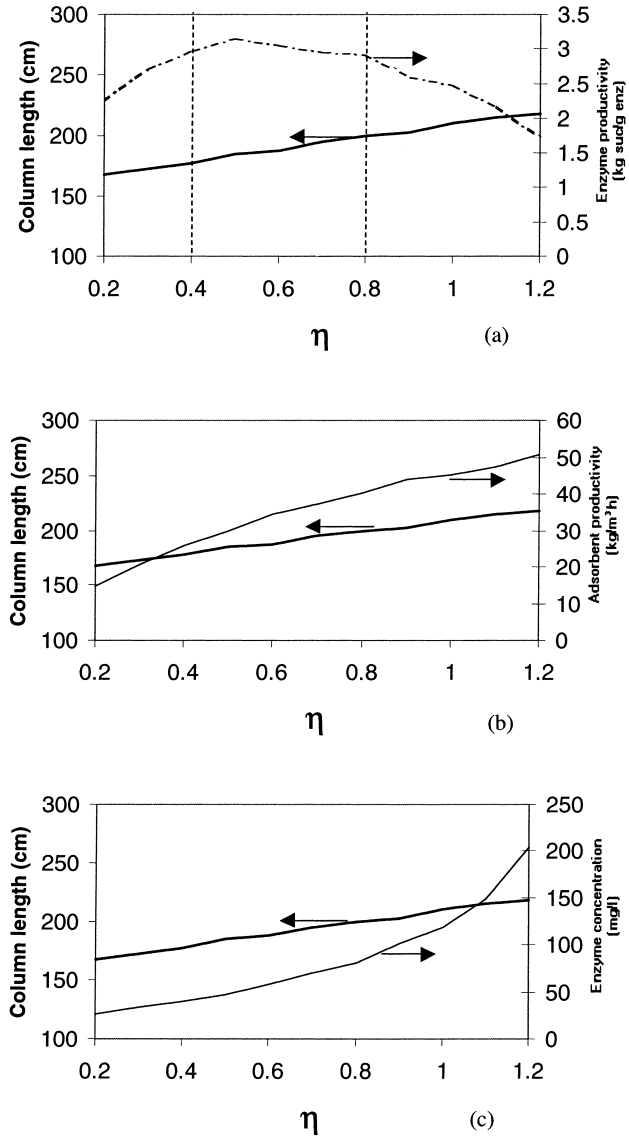

Fig. 4. Results from design algorithm for $\beta = 1.1$. All graphs plot η as a function of minimum length. The secondary vertical axis in each graph stands for enzyme productivity (a); adsorbent productivity (b); minimum required enzyme concentration (c).

One may note that the optimal column lengths obtained in Figs. 4–6 are quite large as compared to the column section area. This is due to the limit on maximum pressure drop at 10 bar per column. This limit was reduced to 5 bar per column. The design algorithm results obtained for $\beta = 1.2$ are shown in Fig. 7. The plateau of maximum enzyme productivity is enlarged to the η interval (0.4, 1.0), although the magnitude of this variable is around 15% less than that obtained for $\Delta P_{max} = 10$ bar per column. Required column lengths are about 40% smaller than those calculated for a higher pressure limit and product dilution is about the same. Energy cost associated with pumping should be confronted with enzyme cost to make a choice for the most profitable column pressure drop, within the packing mechanical strength limitations.

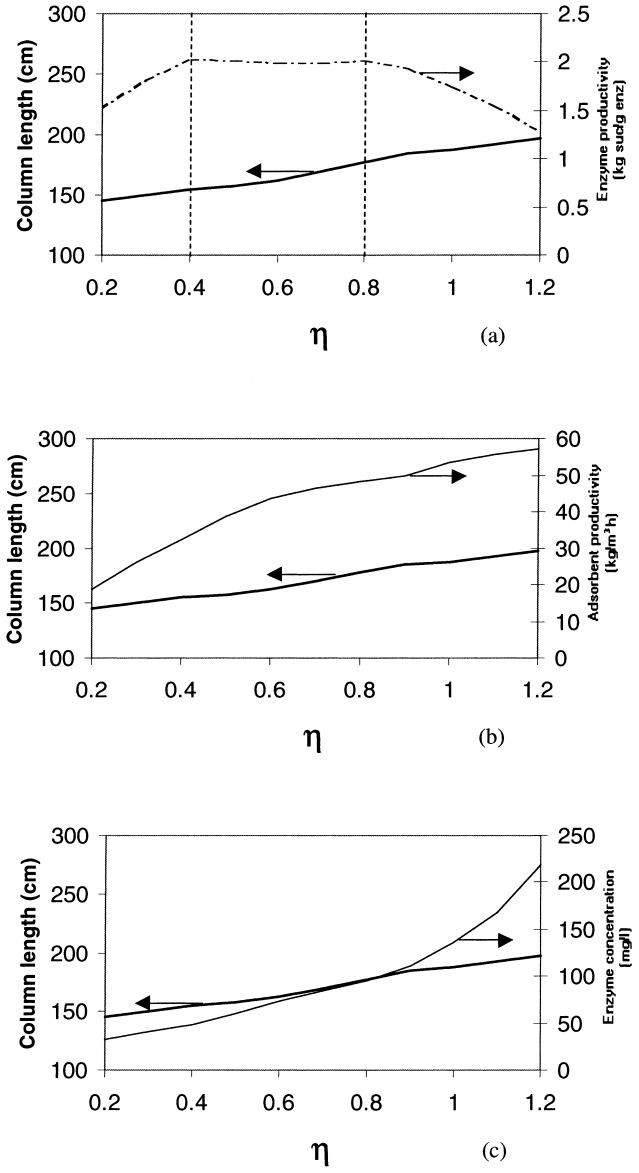

Fig. 5. Results from design algorithm for $\beta = 1.2$. All graphs plot η as a function of minimum length. The secondary vertical axis in each graph stands for enzyme productivity (a); adsorbent productivity (b); minimum required enzyme concentration (c).

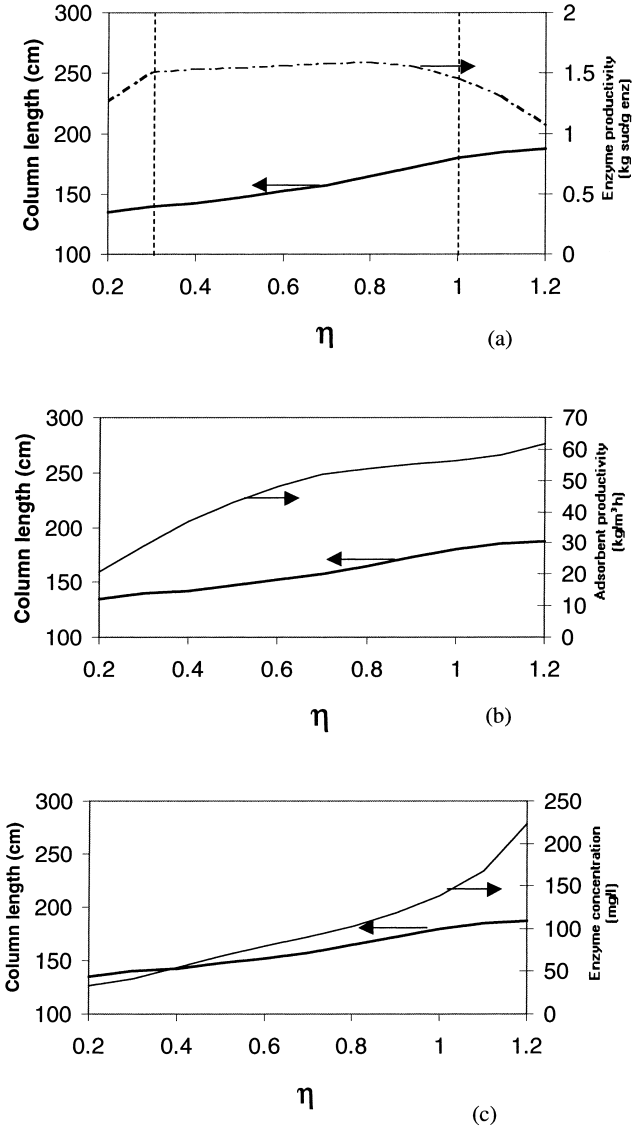

Fig. 6. Results from design algorithm for $\beta = 1.3$. All graphs plot η as a function of minimum length. The secondary vertical axis in each graph stands for enzyme productivity (a); adsorbent productivity (b); minimum required enzyme concentration (c).

Fig. 8(a) shows the optimal (γ_2, γ_3) pairs obtained for $0.2 < \eta < 1.2$ at the four situations previously analysed. It is interesting to observe that the points lie in a common region and have a common trend which may be roughly described by the straight thick line on the figure. The slope of this line is quite different from the line of optimum operation obtained from an equilibrium model for non-reactive SMB's, both shown in Fig. 8. The "path" falls within the area defined for complete separation only for low flowrates.

Table 4
Comparison of design results for various values of safety margin β on γ_1 and γ_4

β	Optimum η range	L_b (cm), D_b (cm)[a]	C_e (mg l^{-1})	Fructose in extract (g l^{-1})	Glucose in raffinate (g l^{-1})
1.1	0.4–0.8	178–200, 6.1–6.5	40–81	67–105	142–237
1.2	0.4–0.8	155–178, 5.7–6.1	48–95	56–90	129–216
1.2[b]	0.4–1.0	107–130, 6.7–7.4	54–137	52–96	116–229
1.3	0.3–1.0	140–180, 5.4–6.1	42–138	38–92	95–233

[a] Column diameter required for a flowrate in Section 1 of 10^3 ml min^{-1}.
[b] Design results obtained for a pressure drop limit of 5 bar per column.

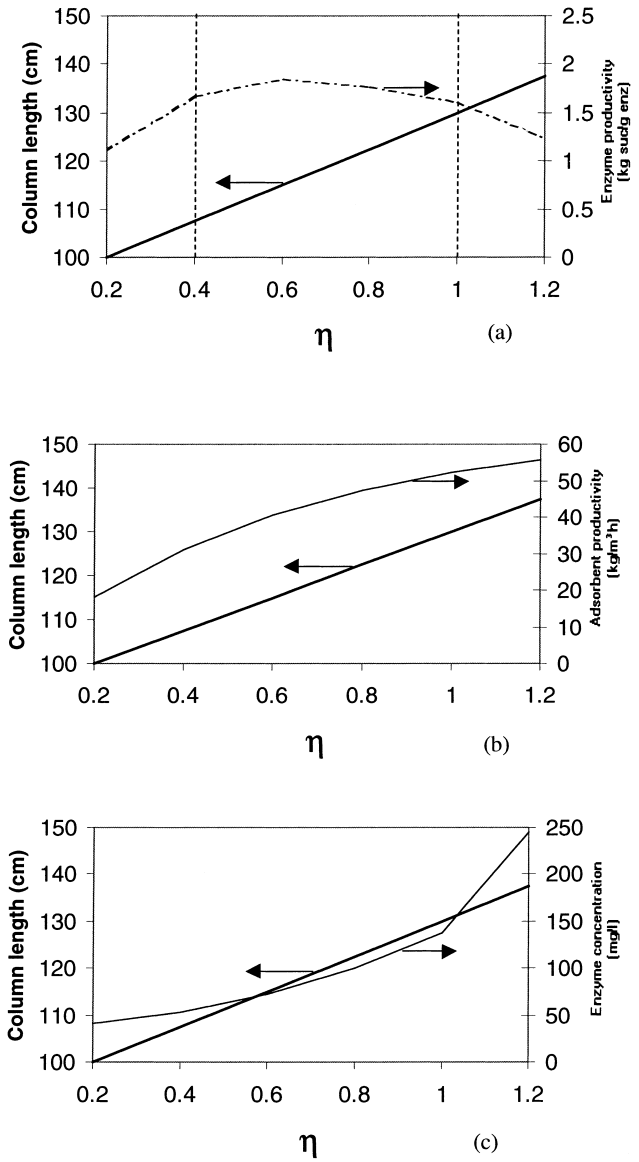

Fig. 7. Results from design algorithm for $\beta = 1.2$. Pressure drop limitation imposed in the design algorithm was 5 bar per column. All graphs plot h as a function of minimum length. The secondary vertical axis in each graph stands for enzyme productivity (a); adsorbent productivity (b); minimum required enzyme concentration (c).

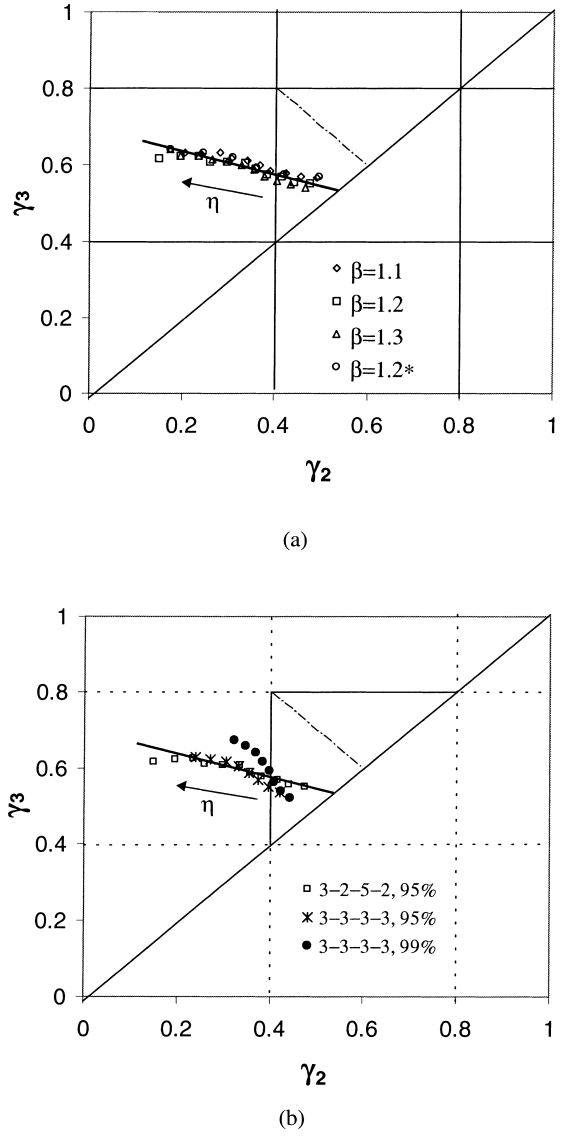

Fig. 8. (a) Optimal operating points (γ_2, γ_3) for β equal to 1.1, 1.2 and 1.3. The data with an asterisk (∗) on the legend stands for the design results obtained with a column pressure drop limit of 5 bar per column. The straight thick line indicates the common trend for all data. The triangle defined by (0.4, 0.4), (0.8, 0.8) and (0.4, 0.8) is that given by the equilibrium model for a non-reactive SMB; (b) optimal operating points for different purity requirements and number of columns per section.

In such cases, one may say that the amount of substrate entering the SMBR is little enough for reaction to take place in a short portion of Section 3 and hence, the SMBR behaves as a SMB. As feed flowrate increases, the path leaves the region of complete separation as defined for a non-reactive SMB. The values of γ_3 seem to approach a new limiting value (at about 0.65), which may be due to the fact that flowrates in Section 3 need to be lower in order to achieve both high conversions and adsorption of fructose, The values of γ_2 violate the restrictions defined for a non-reactive SMB. This would mean that glucose would not be completely dessorbed in Section 2 and hence, would contaminate the extract. The correlation between the inclusion of the reaction and the violation of this condition is not straight-forward. It may also be due to the fact that a little contamination is allowed in our design package. Fig. 8(b) shows results of optimum operation points for $\beta = 1.2$ with different number of columns per section and a different constraint on product purity requirements. Varying the number of columns per section to 3–3–3–3 does not change the path obtained. However, when the purity requirement is 99%, the obtained optimum path deviates from those obtained for 95% purity. Yet, it is quite different form the path for non-reactive SMB's. Reaction parameters may also affect the optimum path and further

Table 5
Comparison between experimental parameters and those obtained from the design algorithm for the same values of feed flowrate, η and β

Parameter	Value used/obtained in the SMBR experiments	Value calculated from design algorithm
L_b (cm)	29	35
A (cm^2)	5.31	4.08
V_b (cm^3)	154	143
C_{enz} ($mg\,l^{-1}$)	250[a]/40[b]	45
Enzyme productivity (kg sucrose per gram enzyme)	0.102[a]/0.636[b]	0.552
(PRX + PRR)/2 ($kg\,m^{-3}\,h^{-1}$)	7.43[a]/7.88[b] (5.05[a]/5.36[b] $kg\,m^{-3}$ per cycle)	8.36 (5.35 $kg\,m^{-3}$ per cycle)
Fructose in extract ($g\,l^{-1}$)	15.78[a]/15.88[b]	15.07
Glucose in raffinate ($g\,l^{-1}$)	22.18[a]/22.61[b]	25.49
t^* (min)	3.4	3.2
γ_2, γ_3	0.45, 0.65[a]; 0.43, 0.63[b]	0.44, 0.64

[a,b] Refer to experiments shown in Fig. 2.

investigation should be done in order to relate them to the non-reactive situation.

The design algorithm was also applied to the conditions of the experiment described in a previous section, i.e. sucrose concentration of $80\,g\,l^{-1}$ in the feed, $\eta = 0.513$, $\beta = 1.2$ (for γ_1) and 1.25 (for γ_4). Pressure drop limitation was set to that measured during the experiment. The results of optimal parameters required to process a feed flowrate of $3.62\,ml\,min^{-1}$ are summarised in Table 5. The required column length is 35 cm, 20% longer than the length of the columns used in our experiment. The section area is smaller so that optimum column volume is approximately the same as the actual column volume. The optimal (γ_2, γ_3) pair is very close to the operating point used in the experiment. In other words, if the columns used in our experiment were 35 cm long, the equipment could convert a feed flowrate of $3.62 \times (5.31/4.08) = 4.71\,ml\,min^{-1}$. The amount of enzyme used in the experiment was 400% overestimated in the first experiment described (Fig. 2(a)). In the experiment reported in Fig. 2(b), enzyme concentration was very close to the ideal value and one may say that the SMBR equipment was operated in nearly optimised conditions for the throughput of $3.62\,ml\,min^{-1}$.

6. Conclusions

A design and optimisation methodology was proposed in this work for the inversion of sucrose and separation of glucose and fructose in a simulated moving bed reactor. The design algorithm used a detailed process model also described in this work. Experimental results obtained were in accordance with simulated results, which validates the proposed model. The design algorithm calculates minimum column lengths and enzyme concentrations, for various values of parameters η and β, which lead to a desired process performance. The constraints on process performance were a minimum reaction conversion of 99% and minimum product purities of 95%. Results from the design algorithm (η, β, L_b, C_e) were used and analysed in the optimisation step by defining enzyme productivity as the objective function to be maximised. Plateaux of enzyme productivities were obtained for η intervals of (0.4, 0.8), at β equal to 1.1 and 1.2, and for the η intervals of (0.3, 1.0) for β equal to 1.3. For a lower column pressure drop limitations, required column lengths are reduced but optimal velocity ratios remain about the same. The final decision on the optimal SMBR operating and geometric conditions may be made by balancing such criteria as robustness, product dilution, energy and enzyme costs. It was also evidenced that the "path" of the optimal operating points (γ_2, γ_3) is the same independently of the safety margin β, on the imposed pressure drop limitations and on the number of columns per section.

Acknowledgements

The authors wish to thank CAPES (proc. 1140/96-5), Ministry of Education of Brazil, for sponsoring Ms. Azevedo's Ph.D. Grant and Project PRAXIS XXI/3.1/CEG/2644/95, Ministry of Science and Technology of Portugal, for providing financial support to this research.

References

[1] P. Cen, G.T. Tsao, Recent advances in the simultaneous bioreaction and product separation processes, Sep. Technol. 3 (1993) 58–75.
[2] M. Meurer, U. Altenhöner, J. Strube, A. Untiedt, H. Schmidt-Traub, Dynamic simulation of a simulated-moving-bed chromatographic reactor for the inversion of sucrose, Starch/Stärke 48 (1996) 452–457.
[3] V. Kruglov, M.C. Bjorklund, R.W. Carr, Optimization of the simulated counter current moving bed chromatographic reactor for the oxidative coupling of methane, Chem. Eng. Sci. 51 (1996) 2945–2950.
[4] M. Kawase, T.B. Suzuki, K. Inoue, K. Yoshimoto, K. Hashimoto, Increased esterification conversion by application of the simulated moving bed reactor, Chem. Eng. Sci. 51 (1996) 2971–2976.
[5] V. Kruglov, Methanol synthesis in a simulated countercurrent moving-bed adsorptive catalytic reactor, Chem. Eng. Sci. 49 (1994) 4699–4716.
[6] G. Ganetsos, P.E. Barker, J.N. Alongwen, Batch and continuous chromatographic systems as combined bioreactor-separators, in: G. Ganetsos, P.E. Barker (Eds.), Preparative and Production Scale Chromatography, Marcell Dekker, New York, 1993, pp. 375–394.

[7] P.E. Barker, G. Ganetsos, J. Ajongwen, A. Akintoye, Bioreaction–separation on continuous chromatographic systems, Chem. Eng. J., Biochem. Eng. J. 50 (1992) B23–B28.
[8] M.R. Sardimi, P.E. Barker, Simultaneous biochemical reaction and separation in a rotating annular chromatograph, Chem. Eng. Sci. 48 (1993) 2613–2615.
[9] K. Hashimoto, S. Adachi, Y. Shirai, Development of new bioreactors of a simulated moving-bed type, in: G. Garetsos, P.E. Barker (Eds). Preparative and production scale chromatography, Marcel Dekker, New York, 1993, pp. 395–419.
[10] M. Mazzotti, G. Storti, M. Morbidelli, Optimal operation of simulated moving bed units for nonlinear chromatographic separations, J. Chromatogr. A 769 (1997) 3–24.
[11] T. Pröll, E. Küsters, Optimisation strategy for simulated moving bed systems, J. Chromatogr. A 800 (1998) 135–150.
[12] C. Heurer, E. Küsters, T. Plattner, A. Seidel-Morgenstern, Design of the simulated moving bed process based on adsorption isotherm measurements using a perturbation method, J. Chromatogr. A 827 (1998) 175–191.
[13] D.C.S. Azevedo, A.E. Rodrigues, Design of a simulated moving bed in the presence of mass transfer resistances, AIChE J. 45 (1999) 956–966.
[14] J. Fricke, M. Meurer, J. Dreisörner, H. Schmidt-Traub, Effect of process parameters on the performance of a simulated moving bed chromatographic reactor, Chem. Eng. Sci. 54 (1999) 1487–1492.
[15] C. Migliorini, M. Fillinger, M. Mazzotti, M. Morbidelli, Analysis of simulated moving-bed reactors, Chem. Eng. Sci. 54 (1999) 2475–2480.
[16] G. Biressi, O. Ludemann-Hombourger, M. Mazzotti, R.-M. Nicoud, M. Morbidelli, Design and optimisation of a SMB unit: role of deviations from equilibrium theory, J. Chromatogr. A 876 (2000) 3–15.
[17] K. Hashimoto, S. Adachi, H. Noujima, H. Maruyama, Models for the separation of glucose/fructose mixture using a simulated moving-bed adsorber, J. Chem. Eng. Jpn. 16 (1983) 400–406.
[18] K.N. Lee, W.K. Lee, A theoretical model for the separation of glucose and fructose mixtures by using a semicontinuous chromatographic refiner, Sep. Sci. Technol. 27 (1992) 295–311.
[19] V. Viard, M-L. Lameloise, Modelling glucose–fructose separation by adsorption chromatography on ion exchange resins, J. Food Eng. 17 (1992) 29–48.
[20] D.C.S. Azevedo, A.E. Rodrigues, Bi-linear driving force approximation in the modeling of simulated moving bed using bidisperse adsorbents, Ind. Eng. Chem. Res. 38 (1999) 3519–3529.
[21] M.M.L. Santos, Produção de dextrano e frutose a partir da sacarose com Leuconostoc Mesenteroids NRRL B512 (f), Ph.D. Thesis, University of Porto, Porto, 2000.
[22] U. Ascher, J. Christiansen, R.D. Russel, Collocation software for boundary-value ODEs, ACM Trans. Math. Software 7 (1981) 209–222.
[23] D.C.S. Azevedo, A.E. Rodrigues, On the obtention of high-fructose solutions from cashew (*Anacardium Occidentale*) apple juice by SMB chromatography, Sep. Sci. Technol. (2000), in press.
[24] D. Thoenes Jr., H. Kramers, Mass transfer from spheres in various regular packings to a flowing fluid., Chem. Eng. Sci. 8 (1958) 271–283.
[25] D.M. Ruthven, C.B. Ching, Countercurrent and simulated countercurrent adsorption separation processes, Chem. Eng. Sci. 44 (1989) 1011–1038.
[26] Ullmann's Encyclopedia of Industrial Chemistry, 6th Edition, Electronic Release, Wiley/VCH, Weinheim, 1999.